Triple-State Dissipative Soliton Laser Via Ultrafast Self-Parametric Amplification

Junsong Peng and Heping Zeng*
State Key Laboratory of Precision Spectroscopy, East China Normal University, Shanghai 200062, China

(Received 5 August 2018; revised manuscript received 26 March 2019; published 22 April 2019)

Laser gains, provided by either stimulated emissions, stimulated scatterings, or nonlinear frequency conversion, exclusively refer to the process in which pump waves transfer their energies to the emitted light. In these cases, the laser field could never acquire gain at the expense of the energy dissipation of itself. We introduce self-parametric amplification, a conceptually different gain mechanism for ultrafast fiber lasers. A prototype ultrafast fiber laser of this kind is realized by combining a standard linear gain with a nonlinear self-parametric gain that supports energy transfer from the spectral tails to the spectral center within the laser field. Remarkably, the ultrafast fiber laser outputs three coexisting dissipative solitons that periodically switch over consecutive round trips with quite different spectra. Our work provides a self-action gain mechanism conducive to developing advanced lasers and could shed light on the Fermi–Pasta–Ulam paradox and breathing soliton dynamics.

DOI: 10.1103/PhysRevApplied.11.044068

I. INTRODUCTION

Generally, stimulated emission in an active gain medium provides the gain required to compensate resonator loss for lasing. There are various gain media that contribute to the development of many different lasers. Various nonlinear optical effects that support energy transfer from pump lasers to intracavity lasing fields can also provide gains, which are widely used to extend the wavelength range of a laser. For example, stimulated scattering processes depending on molecular vibrations and density variations of the medium are widely used as gain mechanisms in Raman and Brillouin lasers, respectively. Recently, a multicolor dissipative-soliton fiber laser has been realized by using double gain mechanisms consisting of stimulated emission and stimulated Raman scattering [1]. Apart from stimulated scattering processes, there is a separate class of nonlinear phenomena called parametric processes in which the energy of the interacting optical field is conserved.

An important class of parametric process refers to the optical Kerr effect, that is, modulation of the refractive index of a medium by light intensity. The Kerr effect relates to a wide range of nonlinear phenomena, such as self-phase modulation (SPM), modulation instability, and four-wave mixing. Generally, these parametric processes can be subdivided into two categories: nonlinear interactions of light requiring external waves (such as four-wave mixing) and those generated by self-action of the propagating optical field, such as SPM and modulation instability [2]. Recently, a new self-action effect called self-parametric amplification (SPA) was found in fiber optics, which manifests itself as optical spectrum narrowing in a passive normal-dispersion fiber [2]. The spectral narrowing refers to the amplification of the central part of the spectrum by energy transfer from the spectral tails. This self-action effect occurs in the continuous wave regime owing to four-wave mixing. Accordingly, in the pulse regime, the interplay between the Kerr effect and dispersion can also give rise to similar spectrum-narrowing phenomena [3]. Although the detailed mechanisms leading to spectrum narrowing are different in the two regimes, spectrum narrowing also belongs to SPA in the pulse regime, as the Kerr effect is involved and no external pump waves are required. To date, SPA only occurs in passive fibers [2,3]. It remains unclear whether it is possible to stimulate SPA gain in a laser. If SPA is activated in an ultrafast fiber laser, an additive gain of the spectral center of the laser field could be achieved at the expense of the spectral tails. This is intrinsically different from standard lasers in which there is no energy transfer within the laser field.

In this work, we demonstrate that SPA-based nonlinear gain can be activated in a mode-locked fiber laser, manifesting itself via the generation of triple-state dissipative solitons. In distinct contrast with standard mode-locked lasers, which emit the same pulses over all round trips, the outputs of the SPA laser periodically switch between three distinctive dissipative solitons. The three dissipative solitons are distinguished by the featured optical spectra, including the double-peaked spectrum from SPM, a single-peaked one from SPA, and a higher-power single-peaked spectrum from erbium-doped fiber (EDF) gain. Recently, switching between two distinctive dissipative solitons was observed in a mode-locked fiber laser [4]. The outputs of the laser periodically switch between two dissipative

*hpzeng@phy.ecnu.edu.cn

solitons with different central spectra. The origin of this switching is different from our laser and refers to the double-minima loss spectrum owing to the birefringent filter inside the laser. The SPA laser on the one hand provides a solution for developing spectral brightness lasers without employing a lossy filter. On the other hand, it refers to an entirely alternative mode-locking regime, showing that the SPA laser can circumvent SPM to some extent.

II. RESULTS AND DISCUSSIONS

A. Mechanisms

When a pulse propagates in a segment of anomalous-dispersion fiber, its spectrum is broadened independent of the initial pulse chirp, since anomalous dispersion tends to shorten the pulse duration leading to enhanced SPM [3,5]. In contrast, in the case of normal-dispersion fiber, an initially negatively chirped pulse can be spectrally compressed after propagating in the fiber. SPM induces a positive chirp in the fiber [6], that is, a frequency downshift of the leading edge and an upshift of the trailing edge of the pulse. As a result, the initial negative chirp of the pulse is compensated by the positive chirp from SPM, leading to a transfer of long and short wavelengths toward the center wavelength (spectral compression) [3]. Note that this spectrum-narrowing effect belongs to SPA, as the central spectrum gains power from the spectral wings without employing an external pump light, and a parametric process is involved (SPM). In particular, if the initial pulse spectrum displays a double-peaked structure (the central parts are, therefore, relatively weak), the intensity increase of the spectral center at the expense of the wings due to SPA makes the amplification of the center even more pronounced.

With the above mechanism in mind, it is straightforward to construct an ultrafast fiber laser with SPA as an additive gain. We emphasize that SPA has never been employed in lasers. The laser set up is shown in Fig. 1(a) (for details, see Appendix A). Nonlinear polarization rotation is employed to achieve mode locking, giving rise to pulse generation [7]. A segment of anomalous-dispersion single-mode fiber (SMF) following the nonlinear polarization rotation section is employed to add a negative chirp to the pulse. Generally, a passive normal-dispersion fiber is required to stimulate SPA; however, in order to realize an integrated set up, a gain fiber with normal dispersion can be employed. Here, normal-dispersion EDF is used, providing both the linear amplification from stimulated emission and nonlinear gain from SPA. Note that normal-dispersion gain fiber has been widely used as a nonlinear attractor for similariton generation [8–11]. Here, the gain fiber is used to provide an alternative function of SPA gain.

B. Simulations

Numerical simulations of the laser model (Fig. 1) are employed to search for the regime in which an additive gain from SPA is activated. Pulse propagation within the fiber sections is modeled with a modified nonlinear Schrödinger equation (NLSE) for the slowly varying pulse envelope

$$\frac{\partial A}{\partial z} = -\frac{1}{2}(i\beta_2)\frac{\partial^2 A}{\partial \tau^2} + i\gamma|A|^2 A + gA. \tag{1}$$

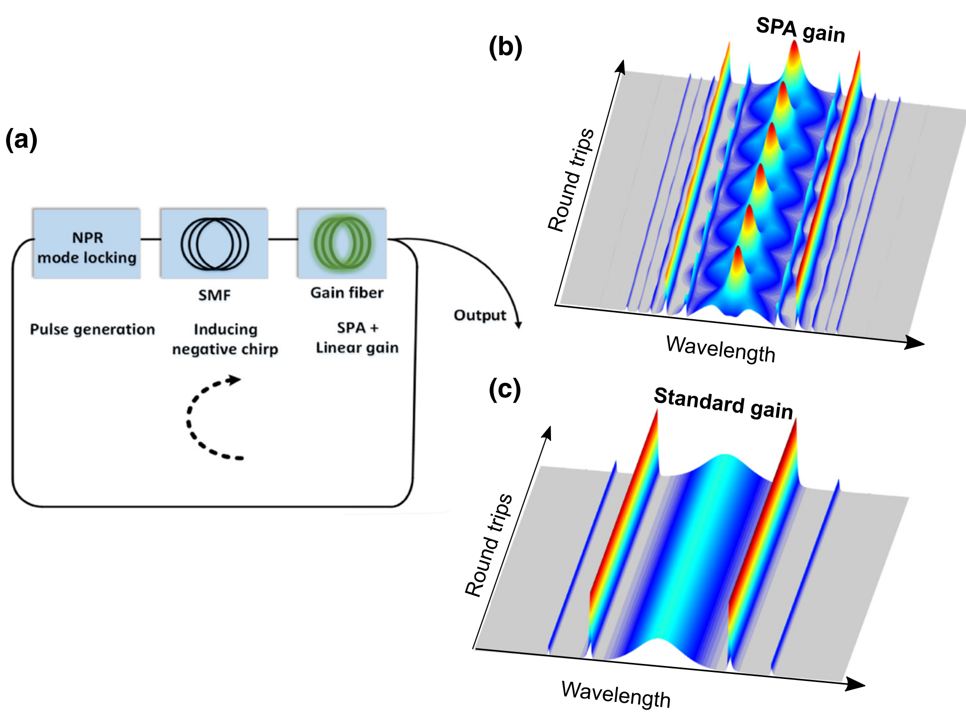

FIG. 1. Schematic diagram of the dissipative-soliton fiber laser with SPA gain. (a) The laser set up. Ultrashort pulses are generated by the well-known mode-locking mechanism—nonlinear polarization rotation (NPR). SMF is employed to add negative chirp to the pulses. The gain fiber provides the linear gain from stimulated emission and nonlinear gain from SPA. The laser can work on two different mode-locking regimes. (b) The standard mode-locking regime. (c) Dynamical spectra are observed when SPA gain is stimulated by controlling the pump power only.

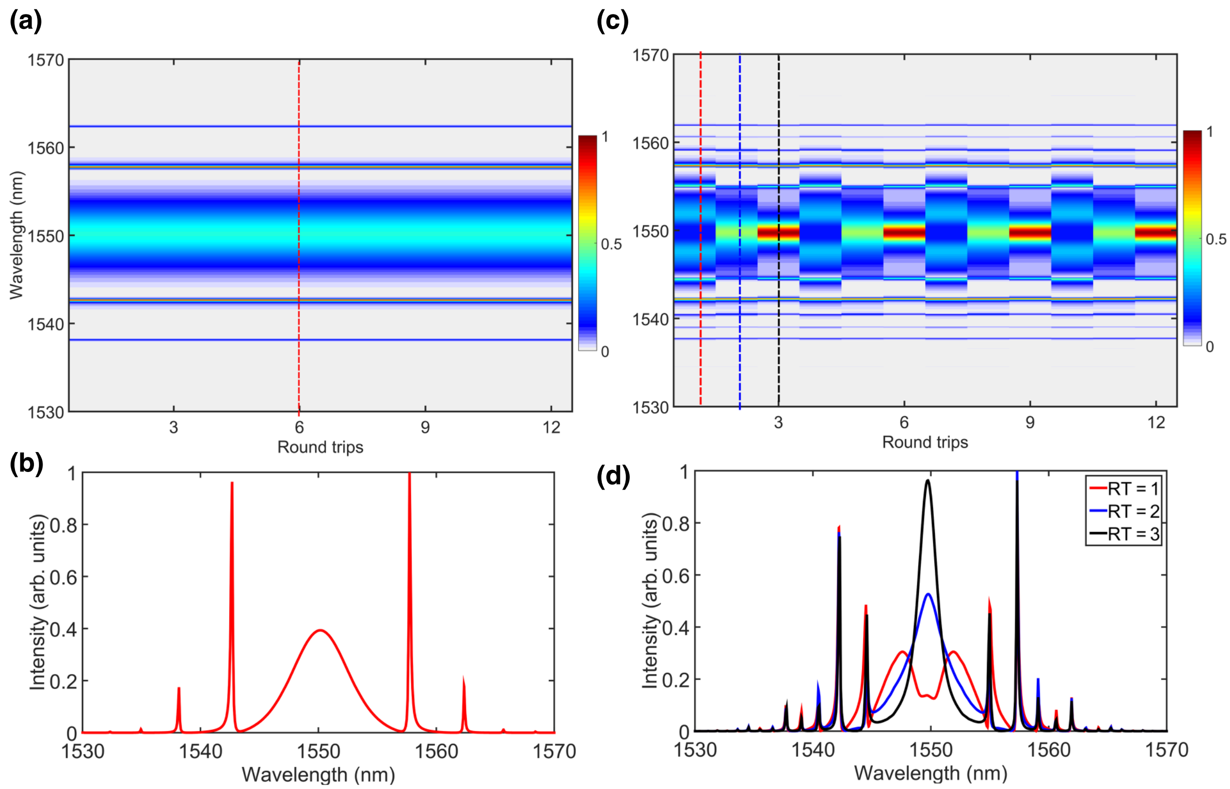

FIG. 2. The spectra of the dissipative solitons at the laser output. (a) The spectra of stable dissipative solitons over consecutive round trips. (b) The detailed spectral profile extracted (cross section) from (a). (c) The spectra of the dissipative solitons when SPA gain is stimulated by increasing the pump power only, exhibiting periodic evolution over consecutive RTs with a period of three RTs. (d) The detailed spectra within one period extracted from (c).

Here, β_2 is the group-velocity delay parameter and γ is the coefficient of cubic nonlinearity for the fiber section. The dissipative terms represent linear gain as well as a Gaussian approximation to the gain profile with the bandwidth Ω. The gain is described by $g = g_0 \exp(-E_P/E_S)$, where g_0 is the small-signal gain, which is nonzero only for the gain fiber, E_P is the pulse energy, and E_S is the gain saturation energy determined by the pump power. To initiate and sustain mode locking, a nonlinear polarization rotation technique is used in our experiment. Here, the mode-locking technique is modeled by a simple transfer function for the sake of clarity: $T = R_0 + \Delta R[1 - 1/(1 + P/P_0)]$, where R_0 is the unsaturable transmission, ΔR is the saturable transmission, P is the pulse instantaneous power, and P_0 is the saturable power. The input pulse is a weak pulse with a Gaussian profile (the pulse has an energy of 1 pJ and its duration is 1 ps). The parameters used in the numerical model will guide the experimental study (see the parameters used in the simulation in Appendix B). The net dispersion of the laser cavity is -0.23 ps^2.

The simulation results show that the traditional mode-locking regime of the laser can be found under a moderate gain saturation energy (pump power). For example, stable dissipative solitons are generated from the laser when the gain saturation energy is set to be 12 pJ, as shown in Figs. 2(a) and 2(b). The strong spectral sidebands symmetrical to the central spectrum are Kelly sidebands generated by the interference between the dispersive wave and soliton [12].

The output of the laser exhibits drastic changes by only increasing the gain saturation energy, as shown in Fig. 2(c). Remarkably, the spectrum returns to its initial state after every three round trips. Figure 2(d) depicts the detailed structure of the spectra of the dissipative solitons within one period. The spectrum shows a double-peaked structure at round trip (RT) 1 while it shows only a single peak at the next two RTs. Here, the double peaks refer to the broader ones between 1545 and 1555 nm [Fig. 2(d), red], and are not related to the spectral peaks that are Kelly sidebands located in the wings. The temporal intensities of the pulses are also shown (see Appendix C). The spectrum narrowing effect that can be clearly observed by comparing the spectra at RTs 1 and 2 is very similar to that observed in the passive normal-dispersion fibers [2]. In both cases, the spectral center is amplified by gaining power from the double-peaked structures of the spectrum. These spectral dynamics [Figs. 2(c) and 2(d)] imply that SPA could be successfully stimulated in the laser.

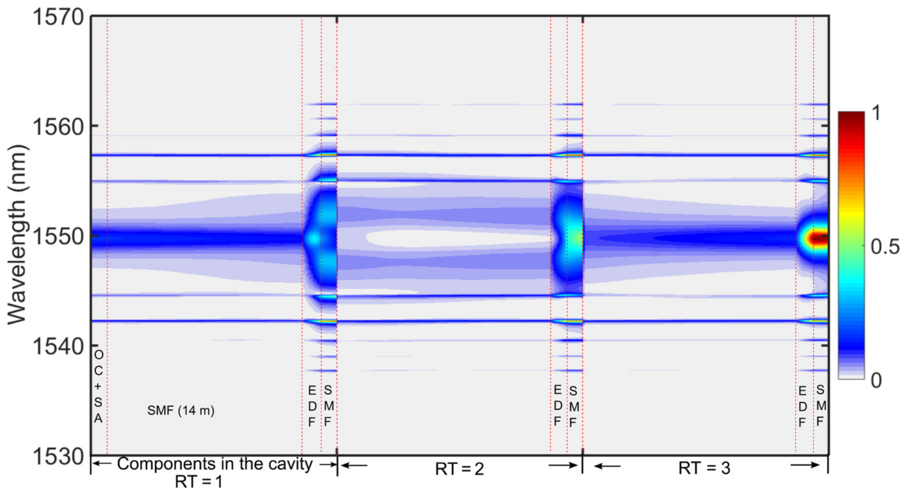

FIG. 3. Intracavity evolution of the pulse spectra over three consecutive RTs (one period). The intracavity components are, in turn, optical coupler (OC), saturable absorber (SA), SMF (14 m), EDF (1.2 m), and SMF from OC (1 m).

To further confirm SPA occurring in the laser, the spectral evolution of the pulse inside each position of the laser is examined. Since the pulse repeats itself every three RTs, its spectral evolutions over three consecutive RTs are investigated. Figure 3 depicts that a double-peaked spectrum [see Fig. 2(d) (red) for the cross-section] occurs owing to SPM in the SMF (after the EDF) in the first RT (RT = 1). The pulse is amplified in the EDF then it is temporally compressed in the following SMF (anomalous dispersion), resulting in strong SPM in the SMF as evidenced by the double-peaked spectrum that is a typical product of SPM [5]. The SPM-induced double structures are well known in ultrafast lasers and amplifier systems [13–15]. Note that the double-peaked structure of the output spectrum of the light source used in Ref. [2] is due to four-wave mixing-induced spectral broadening inside the Raman converter cavity. This leads to a spectral breadth that exceeds the reflection bandwidth of the fiber Bragg grating output coupler, and therefore, leads to radiation “overflowing” the fiber Bragg grating reflector [2].

In the next RT (RT = 2), the double-peaked spectrum preserves its shape in the SMF before the EDF. However, the double peaks approach each other and finally merge to form a single peak in the EDF. Namely, the spectral center is amplified by gaining power from the spectral wings. During the third RT (RT = 3), the single-peak spectrum has no noticeable change until the pulse enters the EDF in which the spectrum is broadened owing to increased energy from amplification in the EDF.

As mentioned above, an initial negative chirp is crucial for SPA to occur. When a pulse with negative chirp propagates in normal-dispersion fiber, the negative chirp is compensated by the positive chirp originating from SPM, resulting in spectrum narrowing of the initial pulse. Therefore, the sign of the pulse chirp before the normal-dispersion fiber reflects to some extent whether the spectrum narrowing originates from SPA in our laser. As shown above (Fig. 3), SPA happens in the EDF in the second RT (RT = 2). Accordingly, we calculate the chirp of the dissipative soliton before entering the EDF in that RT. The chirp is shown in Fig. 4(a) (blue) together with the intensity of the pulse (black). Indeed, the chirp of the dissipative soliton before entering the EDF is negative. After propagating in the EDF, the chirp is significantly reduced and the resulting chirp is slightly positive, as shown in Fig. 4(b) (blue), which depicts the chirp of the pulse at the end of EDF.

The results described above show that the normal-dispersion EDF is the key element supporting SPA in the laser. We also do further simulations in which the normal-dispersion EDF is replaced by EDF with anomalous dispersion. In these cases, SPA does not occur since anomalous dispersion fibers only result in spectral broadening of the input pulses.

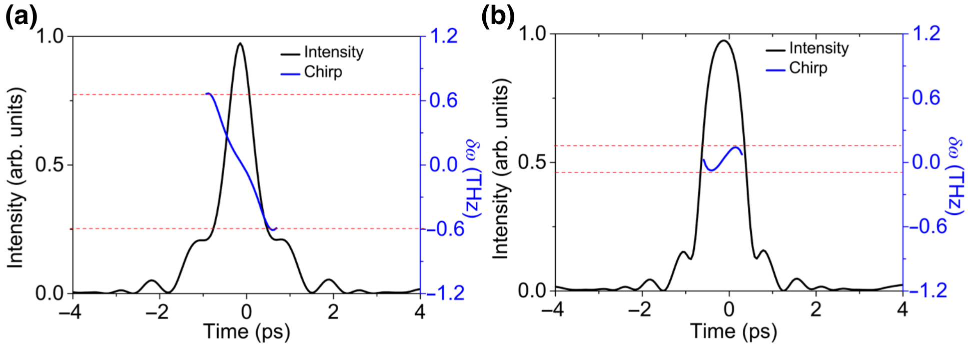

FIG. 4. The parameters of the pulse before and after the EDF in the second RT. (a) The chirp (blue) and temporal intensity (black) of the pulse before the EDF. (b) The chirp (blue) and temporal intensity (black) of the pulse after the EDF.

C. Experiments

We construct an EDF laser with the parameters used in the simulation. The laser could be easily mode locked by nonlinear polarization rotation. The simulation shows that once the laser is mode locked in the standard single-pulsing regime, solely increasing the pump power gives rise to SPA. In accordance with the simulation, during the experiments, the polarization controllers are fixed once mode locking is achieved and only the pump power is varied to search for the regime in which the SPA gain is stimulated.

When the laser is mode locked just above the mode-locking threshold (23.3 mW), stable pulses can be observed. The pulse duration is 590 fs as measured by a commercial autocorrelator. The average output power of the laser is 1.6 mW, corresponding to a dissipative soliton with an energy of 126 pJ. We measure the optical spectra of the pulses in real time by dispersive Fourier transformation (DFT) [16,17]. The DFT technique uses chromatic dispersion to map the spectrum of an optical pulse to a temporal waveform whose intensity profile imitates the pulse spectrum. By virtue of DFT, RT resolved spectra can be measured, which contributes to revealing various fast dynamics in lasers [18–25]. The spectral evolution of the dissipative solitons measured by DFT is depicted in Fig. 5(a). Figure 5(b) shows a single-shot spectrum that is a cross section of Fig. 5(a); since it is a single-shot spectrum, the signal-to-noise ratio is low.

By increasing the pump power only, the energy and spectral width of the dissipative solitons are increased. In these cases, the spectra do not change over consecutive RTs. Remarkably, the spectra periodically switch between three different ones when the pump power is above a threshold of 28 mW, as shown in Fig. 5(c). The spectra change considerably over consecutive RTs. Meanwhile, it follows a periodic evolution with a period of three RTs. The spectra within one period are also shown [Fig. 5(d)]. The experimentally measured spectral dynamics shown in Figs. 5(c) and 5(d) qualitatively agree with the simulation results as shown in Figs. 2(c) and 2(d). First, the period of the spectral evolution (three RTs) is the same for both the experiments and simulations. Second, the detailed evolution within one period is also similar. Both of them show that a double-peaked spectrum is transferred to a single-peak one over the next RT. Third, both the

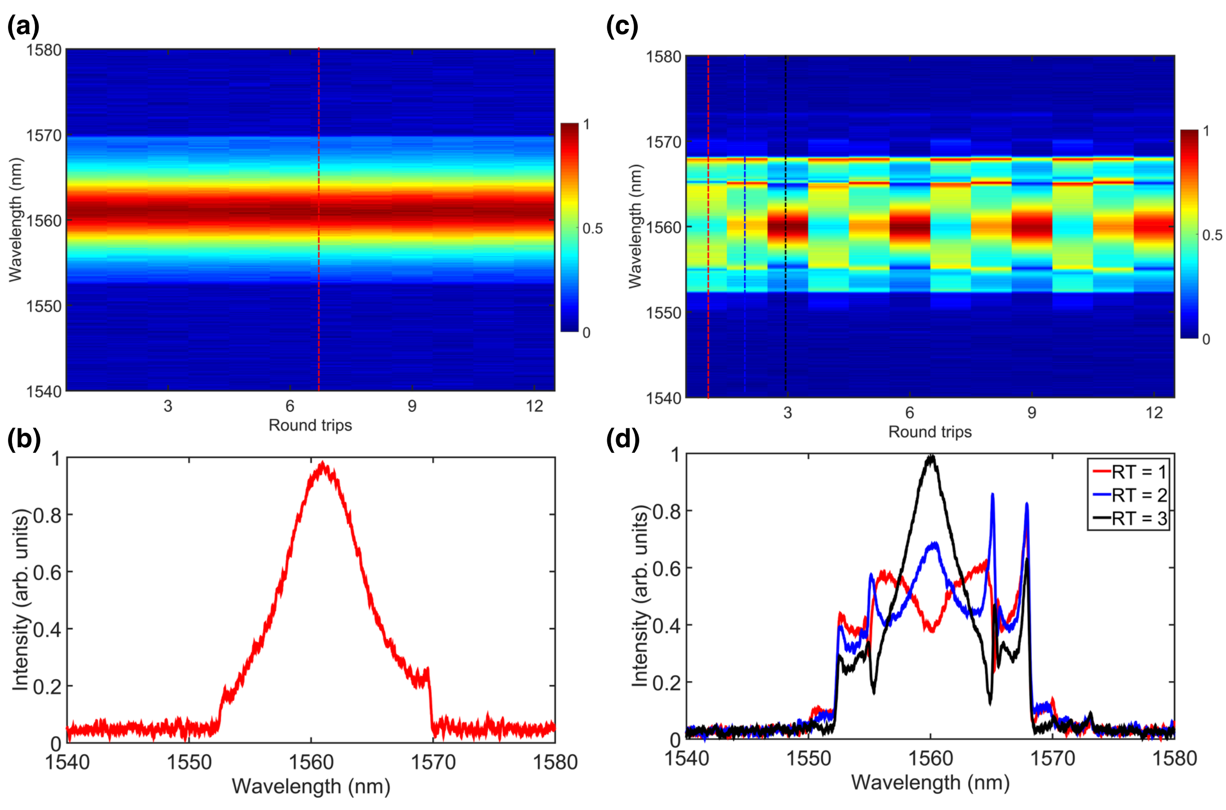

FIG. 5. The experimentally measured (using DFT) optical spectra of the dissipative solitons at the laser output. (a) The spectra of the stable dissipative solitons over consecutive RTs under low pump power (23.3 mW). (b) The spectrum profile extracted from (a). (c) The spectra of the dissipative solitons measured when SPA gain is stimulated by increasing the pump power from 23.3 to 28 mW, exhibiting periodic evolution over consecutive RTs with a period of three RTs. (d) The detailed spectra extracted from (c) showing the structures of the spectra. These spectral dynamics qualitatively agree with the numerical results presented in Fig. 2.

simulations and experiments show that SPA has a threshold effect. Under the threshold, conventional mode-locked pulses are generated and SPA occurs when the pump power is above the threshold. In fact, the threshold relates to the SPM-induced spectrum broadening that has a threshold as observed in many ultrafast optics systems [13–15]. Once the spectrum broadening occurs, SPA acts to narrow the spectrum in the next RT such that the pulse evolution is self-consistent in the laser, showing the virtue of self-adaption of the laser to strong SPM. This alternative laser regime only exists in a narrow pump power range, which is 0.7 mW. A further increase in pump power makes the laser switch to continuous wave emission. The Kelly sidebands observed in the simulations are much stronger than those in the experiments. This is probably due to incomplete knowledge of the parameters of the saturable absorber (nonlinear polarization rotation).

It is well known that the increment of pump power enhances SPM in ultrafast lasers, causing a single pulse to break up into multiple pulses [26], noiselike pulses [27], or soliton explosions [28–32]. Our work shows that in addition to these well-known dynamics, SPA can be stimulated, resulting in vastly different laser dynamics: triple-state dissipative soliton switching. Such dynamics is inherently different from the spectra evolution observed in the build-up phase of dissipative solitons in an ultrafast fiber laser [33]. In the latter case, the dynamic spectra finally become modulated, representing the generation of bound solitons. Our work is also different from multiple-period soliton pulsation in passively mode-locked fiber lasers in which periodic energy evolution was observed [34,35].

The dissipative soliton dynamics shown above resembles that of breathing solitons in microresonators [36,37]. The broadening and subsequent splitting of the soliton spectrum [37], as well as the energy transfer between the soliton spectral center and wings [36] observed in the microresonators are also observed in our laser. In addition, the transition from stationary mode locking to periodical triple-state dissipative soliton mode locking by an increase in the pump power is the same as those obtained in breather solitons in microresonators [36,37]. Such a transition results from the well-known Hopf bifurcation [37,38]. It is remarkable that the two distinct systems can have similar soliton dynamics, suggesting the universality of such a phenomenon. Nevertheless, there are differences between the two systems. First, the origins are different. The periodical spectral dynamics observed in the microresonators is characteristic of breathing solitons. The similar dynamics observed in our laser arise from a cascade process including linear gain, self-phase modulation, and self-parametric gain-induced spectrum narrowing. Second, the governing equations are different. A Lugiato-Lefever equation governs the dynamics of microresonators, while a discrete model based on a modified nonlinear Schrödinger equation governs our laser dynamics. The latter is much more complex as it considers more physical effects including gain, gain dispersion, and the mode-locking mechanism. Third, the microresonators have anomalous dispersion while our laser requires a dispersion-managed cavity with a segment of anomalous-dispersion fiber to provide negative chirp such that self-parametric gain is triggered in the normal-dispersion fiber.

Our work can have practical applications. SPM, a well-known adverse nonlinear effect in ultrafast fiber lasers, was previously avoided mainly by using large-mode-area fiber (compromised by beam quality, integrity, and costs), but could now be readily overcome by SPA in SMF to some extent. Indeed, our result shows that the double-peaked spectrum resulting from SPM can be effectively shaped to a single-peak one. In addition, our work is performed in the spectral domain, and could be possibly extended to the spatial domain. Spatial SPM degrades the quality of optical beams (for instance, a Gaussian beam suffers from ring patterns due to spatial SPM), but a good-quality beam may be generated by deploying spatial SPA. Finally, the switching between three distinctive dissipative solitons represents an alternative type of instability that limits the power scaling of mode-locked lasers. Our work suggests that excluding the use of anomalous dispersion fibers in a laser can eliminate SPA since the negative chirp generated by such fibers is required for SPA to occur.

III. CONCLUSION

Our laser showing switching between three distinctive dissipative solitons because of cascade nonlinear processes including SPM and SPA brings important insights into dissipative solitons. In the broader context, triple-state dissipative soliton switching could be universal in ultrafast lasers. Observations of their existence in different laser systems such as Ti:sapphire and semiconductor lasers are thus of particular interest. In addition, the NLSE is used to simulate the dynamics in our laser. Importantly, the NLSE is a universal model describing many different physical systems, such as Bose-Einstein condensates [39], hydrodynamics, and plasmas [40]. Therefore, the rich dynamics of dissipative solitons we observe are not limited to optics and might also be present in many physical systems.

ACKNOWLEDGMENTS

This work was supported by National Key Research and Development Program (Grant No. 2018YFB0407100), National Natural Science Fund of China (Grants No. 11434005, No. 11727812, No. 11621404, No. 11561121003, No. 61775059, and No. 11704123), Key Project of Shanghai Education Commission (Grant No. 2017-01-07-00-05-E00021), and Science and Technology Innovation Program of Basic Science Foundation of Shanghai (Grant No. 18JC1412000).

APPENDIX A: THE LASER SET UP

The detailed laser set up is shown in Fig. 6. A 1.2-m long segment of EDF is used as the gain medium. This fiber is pumped through a 980/1550 nm wavelength division multiplexer (WDM) by a 976-nm laser diode. Nonlinear polarization rotation is employed to achieve mode locking due to its relatively simple experimental realization: an in-fiber polarization-dependent isolator (PDI) sandwiched between two polarization controllers (PCs) converts nonlinear polarization rotation to amplitude modulation, initiating and stabilizing mode-locked operation, while also ensuring unidirectional oscillation. A 30:70 fiber coupler is employed to tap 30% of the laser power out of the cavity.

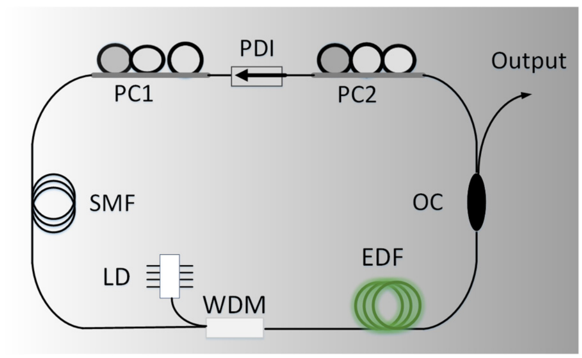

FIG. 6. The detailed schematic diagram of the dissipative soliton fiber laser. LD—laser diode; WDM—wavelength-division multiplexer; EDF—erbium-doped fiber; OC—optical coupler; PC—polarization controller; PDI—polarization-dependent isolator; SMF—single-mode fiber.

APPENDIX B: THE PARAMETERS USED IN THE SIMULATION

The parameters used in the simulations are shown in the table below. The simulations are carried out using split-step Fourier method.

OC	SA	SMF (SMF28)	EDF (OFS 80)	SMF (Nufern 980)
$T = 0.3$	$R_0 = 0.5$	$\beta_2 = -0.021$ ps^2/m	$\beta_2 = 0.064$ ps^2/m	$\beta_2 = -0.0114$ ps^2/m
	$\Delta R = 0.4$	$\gamma = 0.00165$ (W m)$^{-1}$	$g = 20$/m	$\gamma = 0.00165$ (W m)$^{-1}$
	$P_0 = 200$ W	$L = 13$ m	$\Omega = 40$ nm $L = 1.2$ m $\gamma = 0.0066$ (W m)$^{-1}$ $E_s = 12$ and 15 pJ (for standard and SPA gain, respectively)	$L = 2$ m

SA: saturable absorber; OFS: optical fiber solutions.

APPENDIX C: THE TEMPORAL PROFILES OF THE TRIPLE-STATE DISSIPATIVE SOLITON

The temporal intensity profiles of the dissipative solitons within one period are also investigated by numerical simulations as shown in Fig. 7. The spectra gradually narrow down from RT 1 to RT 3 [Fig. 2(d)], implying the increasing of the pulse durations as illustrated in Fig. 7.

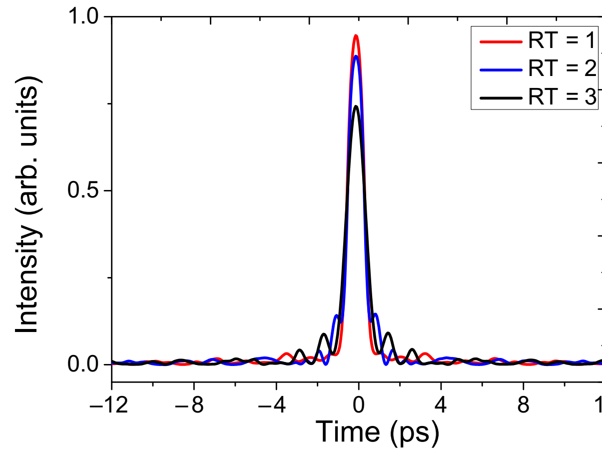

FIG. 7. The temporal profiles of the dissipative solitons over consecutive RTs when SPA gain is stimulated.

[1] S. A. Babin, E. V. Podivilov, D. S. Kharenko, A. E. Bednyakova, M. P. Fedoruk, V. L. Kalashnikov, and A. Apolonski, Multicolour nonlinearly bound chirped dissipative solitons, Nat. Commun. **5**, 4653 (2014).

[2] S. K. Turitsyn, A. E. Bednyakova, M. P. Fedoruk, S. B. Papernyi, and W. R. L. Clements, Inverse four-wave mixing and self-parametric amplification in optical fibre, Nat. Photonics **9**, 608 (2015).

[3] S. Planas, N. P. Mansur, C. B. Cruz, and H. Fragnito, Spectral narrowing in the propagation of chirped pulses in single-mode fibers, Opt. Lett. **18**, 699 (1993).

[4] C. Bao, W. Chang, C. Yang, N. Akhmediev, and S. T. Cundiff, Observation of Coexisting Dissipative Solitons in a Mode-Locked Fiber Laser, Phys. Rev. Lett. **115**, 253903 (2015).

[5] G. P. Agrawal, *Nonlinear Fiber Optics* (Academic Press, New York, 2007).

[6] W. Tomlinson, R. H. Stolen, and A. M. Johnson, Optical wave breaking of pulses in nonlinear optical fibers, Opt. Lett. **10**, 457 (1985).

[7] K. Tamura, H. A. Haus, and E. P. Ippen, Self-starting additive pulse mode-locked Erbium fiber ring laser, Electron. Lett. **28**, 2226 (1992).

[8] M. E. Fermann, V. I. Kruglov, B. C. Thomsen, J. M. Dudley, and J. D. Harvey, Self-Similar Propagation and Amplification of Parabolic Pulses in Optical Fibers, Phys. Rev. Lett. **84**, 6010 (2000).

[9] F. O. Ilday, J. R. Buckley, W. G. Clark, and F. W. Wise, Self-Similar Evolution of Parabolic Pulses in a Laser, Phys. Rev. Lett. **92**, 213902 (2004).

[10] B. Oktem, C. Ulgudur, and F. O. Ilday, Soliton-similariton fibre laser, Nat. Photonics **4**, 307 (2010).

[11] J. Peng, L. Zhan, T. Chen, Z. Gu, K. Qian, S. Luo, and Q. Shen, All-fiber ultrashort similariton generation, amplification, and compression at telecommunication band, J. Opt. Soc. Am. B **29**, 2270 (2012).

[12] S. Kelly, Characteristic sideband instability of periodically amplified average soliton, Electron. Lett. **28**, 806 (1992).

[13] Z. Zhao, B. M. Dunham, and F. W. Wise, Generation of 150 W average and 1 MW peak power picosecond pulses from a rod-type fiber master oscillator power amplifier, J. Opt. Soc. Am. B **31**, 33 (2014).

[14] R. Lindberg, P. Zeil, M. Malmström, F. Laurell, and V. Pasiskevicius, Accurate modeling of high-repetition rate ultrashort pulse amplification in optical fibers, Sci. Rep. **6**, 34742 (2016).

[15] W. Fu, L. G. Wright, and F. W. Wise, High-power femtosecond pulses without a modelocked laser, Optica **4**, 831 (2017).

[16] K. Goda and B. Jalali, Dispersive Fourier transformation for fast continuous single-shot measurements, Nat. Photonics **7**, 102 (2013).

[17] K. Goda, D. R. Solli, K. K. Tsia, and B. Jalali, Theory of amplified dispersive Fourier transformation, Phys. Rev. A **80**, 043821 (2009).

[18] A. F. Runge, C. Aguergaray, N. G. Broderick, and M. Erkintalo, Coherence and shot-to-shot spectral fluctuations in noise-like ultrafast fiber lasers, Opt. Lett. **38**, 4327 (2013).

[19] G. Herink, F. Kurtz, B. Jalali, D. R. Solli, and C. Ropers, Real-time spectral interferometry probes the internal dynamics of femtosecond soliton molecules, Science **356**, 50 (2017).

[20] K. Krupa, K. Nithyanandan, U. Andral, P. Tchofo-Dinda, and P. Grelu, Real-Time Observation of Internal Motion within Ultrafast Dissipative Optical Soliton Molecules, Phys. Rev. Lett. **118**, 243901 (2017).

[21] A. Mahjoubfar, D. V. Churkin, S. Barland, N. Broderick, S. K. Turitsyn, and B. Jalali, Time stretch and its applications, Nat. Photonics **11**, 341 (2017).

[22] G. Herink, B. Jalali, C. Ropers, and D. R. Solli, Resolving the build-up of femtosecond mode-locking with single-shot spectroscopy at 90 MHz frame rate, Nat. Photonics **10**, 321 (2016).

[23] K. Krupa, K. Nithyanandan, and P. Grelu, Vector dynamics of incoherent dissipative optical solitons, Optica **4**, 1239 (2017).

[24] P. Ryczkowski, M. Närhi, C. Billet, J. M. Merolla, G. Genty, and J. M. Dudley, "Real-time full-field characterization of transient dissipative soliton dynamics in a mode-locked laser," Nat. Photonics 12 221 (2018).

[25] J. Peng and H. Zeng, Build-up of dissipative optical soliton molecules via diverse soliton interactions, Laser Photonics Rev. **12**, 1800009 (2018).

[26] D. Y. Tang, L. M. Zhao, B. Zhao, and A. Q. Liu, Mechanism of multisoliton formation and soliton energy quantization in passively mode-locked fiber lasers, Phys. Rev. A **72**, 43816 (2005).

[27] M. Horowitz, Y. Barad, and Y. Silberberg, Noiselike pulses with a broadband spectrum generated from an erbium-doped fiber laser, Opt. Lett. **22**, 799 (1997).

[28] J. M. Soto-Crespo, N. Akhmediev, and A. Ankiewicz, Pulsating, Creeping, and Erupting Solitons in Dissipative Systems, Phys. Rev. Lett. **85**, 2937 (2000).

[29] S. T. Cundiff, J. M. Soto-Crespo, and N. Akhmediev, Experimental Evidence for Soliton Explosions, Phys. Rev. Lett. **88**, 073903 (2002).

[30] A. F. Runge, N. G. Broderick, and M. Erkintalo, Observation of soliton explosions in a passively mode-locked fiber laser, Optica **2**, 36 (2015).

[31] M. Liu, A.-P. Luo, Y.-R. Yan, S. Hu, Y.-C. Liu, H. Cui, Z.-C. Luo, and W.-C. Xu, Successive soliton explosions in an ultrafast fiber laser, Opt. Lett. **41**, 1181 (2016).

[32] J. Peng and H. Zeng, Soliton collision induced explosions in a mode-locked fibre laser, Commun. Phys. **2**, 34 (2019).

[33] J. Peng, M. Sorokina, S. Sugavanam, N. Tarasov, D. V. Churkin, S. K. Turitsyn, and H. Zeng, Real-time observation of dissipative soliton formation in nonlinear polarization rotation mode-locked fibre lasers, Commun. Phys. **1**, 20 (2018).

[34] J. M. Soto-Crespo, M. Grapinet, P. Grelu, and N. Akhmediev, "Bifurcations and multiple-period soliton pulsations in a passively mode-locked fiber laser," Phys. Rev. E **70**, 066612 (2004).

[35] J. Soto-Crespo, P. Grelu, and N. Akhmediev, Dissipative rogue waves: Extreme pulses generated by passively mode-locked lasers, Phys. Rev. E **84**, 016604 (2011).

[36] C. Bao, J. A. Jaramillo-Villegas, Y. Xuan, D. E. Leaird, M. Qi, and A. M. Weiner, "Observation of Fermi-Pasta-Ulam Recurrence Induced by Breather Solitons in an Optical Microresonator," Phys. Rev. Lett. **117** 163901 (2016).

[37] E. Lucas, M. Karpov, H. Guo, M. L. Gorodetsky, and T. J. Kippenberg, Breathing dissipative solitons in optical microresonators, Nat. Commun. **8**, 736 (2017).

[38] F. Leo, L. Gelens, P. Emplit, M. Haelterman, and S. Coen, Dynamics of one-dimensional Kerr cavity solitons, Opt. Express **21**, 9180 (2013).

[39] J. H. V. Nguyen, D. Luo, and R. G. Hulet, Formation of matter-wave soliton trains by modulational instability, Science **356**, 422 (2017).

[40] E. Kuznetsov, A. Rubenchik, and V. E. Zakharov, Soliton stability in plasmas and hydrodynamics, Phys. Rep. **142**, 103 (1986).